arXiv:2211.14597v2 [cond-mat.mes-hall] 11 Jan 2023

Temperature dependence of the energy band gap in $ZrTe_5$: implications for the topological phase

I. Mohelsky,[1] J. Wyzula,[2] B. A. Piot,[1] G. D. Gu,[3] Q. Li,[3,4] A. Akrap,[2] and M. Orlita[1,5,*]

[1] *Laboratoire National des Champs Magnétiques Intenses, LNCMI-EMFL, CNRS UPR3228, Univ. Grenoble Alpes, Univ. Toulouse, Univ. Toulouse 3, INSA-T, Grenoble and Toulouse, France*

[2] *Department of Physics, University of Fribourg, Chemin du Musée 3, 1700 Fribourg, Switzerland*

[3] *Condensed Matter Physics and Materials Science Division, Brookhaven National Laboratory, Upton, New York 11973-5000, USA*

[4] *Department of Physics and Astronomy, Stony Brook University, Stony Brook, NY 11794-3800, USA*

[5] *Faculty of Mathematics and Physics, Charles University, Ke Karlovu 5, Prague, 121 16, Czech Republic*

(Dated: January 12, 2023)

Using Landau level spectroscopy, we determine the temperature dependence of the energy band gap in zirconium pentatelluride ($ZrTe_5$). We find that the band gap reaches $E_g = (5\pm1)$ meV at low temperatures and increases monotonously when the temperature is raised. This implies that $ZrTe_5$ is a weak topological insulator, with non-inverted ordering of electronic bands in the center of the Brillouin zone. Our magneto-transport experiments performed in parallel show that the resistivity anomaly in $ZrTe_5$ is not connected with the temperature dependence of the band gap.

Zirconium pentatelluride ($ZrTe_5$) is a narrow-gap system widely explored in the past [1–4], often in the context of so-called resistivity anomaly [5–10]. More recently, theoretical studies of $ZrTe_5$ that were primarily focused on topological properties induced a renewed interest in this system. In particular, the $ZrTe_5$ monolayer was proposed to be a large-gap quantum spin Hall insulator [11]. Over the past few years, a number of experiments has been performed on bulk and thin layers of $ZrTe_5$ and expanded our knowledge about this material considerably. The experimentally observed phenomena in $ZrTe_5$ comprise the magneto-chiral effect [12, 13], the giant planar Hall effect [14], the quasi-quantized quantum Hall effect [15, 16], pressure-induced superconductivity [17], or optical conductivity that is linear in photon energy [18, 19].

This series of important experimental observations contrasts with our current understanding of low-energy excitations in $ZrTe_5$. In fact, no consensus has been so far established whether the electronic bands in bulk $ZrTe_5$ have normal or inverted ordering, *i.e.*, whether this material is a strong or weak topological insulator (STI or WTI). Ab initio calculations favor the STI phase [20], but their prediction force may be limited in a system close to the topological phase transition. Experimentally, both STI and WTI phases have been reported, see Refs. [13, 21–25] and [26–30], respectively, based on transport, ARPES and optical data.

In this work, we explore, using THz/infrared magneto-spectroscopy, the temperature dependence of the band gap in $ZrTe_5$, in order to test the topological phase of this material. We find that the gap is non-zero at low temperatures, $E_g = (5 \pm 1)$ meV at $T = 5$ K, and it increases with T monotonously. Such behaviour is consistent with $ZrTe_5$ being a weak topological insulator.

Our experiments were performed on bulk $ZrTe_5$ synthesized using self-flux growth [12]. The explored sample was attached using GE varnish to a metallic holder that was covered by a thin paper sheet, and surrounded by the helium exchange gas. The temperature was controlled locally, using a heating coil, and measured by two Cernox thermometers placed at two different locations nearby the sample. A relatively large thickness of the sample (≈0.5 mm) was chosen to avoid effects related to the temperature-induced strain. Results obtained on this sample, presented here, were reproduced on several other specimens with different thicknesses, and glued in different configurations.

We measured relative magneto-reflectivity, R_B/R_0, in the Faraday configuration, *i.e.*, with the wave vector of light propagating parallel to the magnetic field aligned with the b crystallographic axis. The radiation of a globar was analyzed by the Bruker Vertex 80v Fourier-transform spectrometer and delivered via light-pipe optics to the sample located in a superconducting coil. A part of the reflected signal was deflected towards an external bolometer, using a silicon beamsplitter. In addition, magneto-transport data were collected in-situ, *i.e.*, in parallel with magneto-optical measurements. To this end, electric contacts were created using graphite paste in a standard 4-contact configuration.

An illustration of the collected magneto-reflectivity data is presented in Fig. 1. It comprises relative magneto-reflectivity, R_B/R_0, measured at $T = 80$ K plotted (a) in a form of a stacked-plot of spectra taken at selected values of B, and (b) as a false-color map. The observed response is in line with preceding magneto-optical studies of $ZrTe_5$ [19, 22, 31, 32]. It closely resembles the magneto-optical response of Landau-quantized electrons in a conical band [33], nevertheless, the characteristic $\sqrt{B}$ dependence of inter-LL excitations is here only approximate. The observed transitions extrapolate to a non-zero

* milan.orlita@lncmi.cnrs.fr

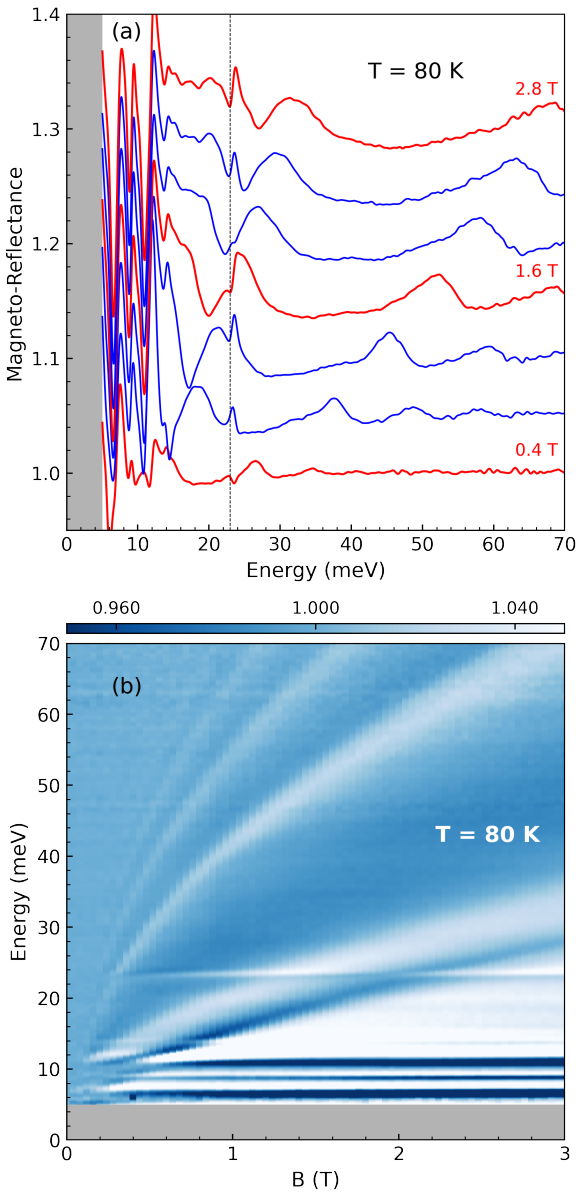


FIG. 1. (a) Stacked-plot of relative magneto-reflectivity spectra, $R_B(\omega)/R_0(\omega)$, collected on $ZrTe_5$ at $T = 80$ K and plotted for selected values of B. (b) the false-color plot of R_B/R_0 plotted with a step of 40 mT. Weakly B-dependent features, nearly horizontal in the plot are phonons, accompanied at low energies (below 10 meV) by an interference pattern. This appears since $ZrTe_5$ becomes transparent at low energies when a sufficiently strong magnetic field is applied. The vertical line in (a) at 23 meV shows the position of the most pronounced phonon mode in $ZrTe_5$ [18].

energy in the limit of vanishing B, thus indicating a band gap in $ZrTe_5$.

To extract the band gap, we have plotted and examined the first field-derivative of the collected spectra, $d/dB[R_B/R_0]$, (Fig. 2a-e) and associated the corresponding maxima with energies of individual inter-LL resonances. This approach is applicable for absorption lines on a positive dielectric background. When additional dissipative processes appear in the background, the position of the resonance may be shifted from the inflection point of $R_B(\omega)/R_0(\omega)$ towards the maximum. This uncertainty increases the error bar of the below extracted/discussed values of the velocity parameter, but has a minor influence on the width of the band gap – the main target of our analysis.

To understand the observed response in the simplest possible manner, we neglect the relatively flat dispersion of electrons along the magnetic field (b axis in our case), see Ref. [19] and interpret our data in terms of excitations in the spectrum of two-dimensional Landau-quantized massive Dirac electrons: $E_n^{\pm} = \pm\sqrt{\Delta^2 + v^2 2e\hbar n B}$ where $n = 0, 1, 2 \ldots$. Here v stands for the velocity parameter averaged in the plane perpendicular to $\mathbf{B}$ (a-c plane) and $+(-)$ refers to the conduction (valence) band. The band gap corresponds to the value of $E_g = 2\Delta$.

The conventional selection rules for electric-dipole transitions, $n \rightarrow n \pm 1$, imply the existence of a series of interband inter-LL excitations: $E^+_{n+1(n)} - E^-_{n(n+1)} = \sqrt{\Delta^2 + v^2 2e\hbar B n} + \sqrt{\Delta^2 + v^2 2e\hbar B(n+1)}$. In our data, such transitions are visible for $n = 0, 1, 2, 3$ and 4. In addition, cyclotron resonance (CR) absorption appears. In a weakly electron-doped sample, only the fundamental CR mode of electrons ($0^+ \rightarrow 1^+$) is active at low temperatures, at the energy of $\sqrt{\Delta^2 + v^2 2e\hbar B} - \Delta$. At elevated temperatures, the fundamental CR mode of holes ($1^- \rightarrow 0^-$) emerges as well, at the same photon energy. In contrast to a preceding study [34], we did not observed any series of excitations that would indicate another gap. The outlined massive Dirac model was used to fit the low-B part of the data (below 1 T), see Fig. 2f-j. This is due to Zeeman effect, which scales linearly with B and which starts to impact visibly the magneto-optical response of $ZrTe_5$ at higher magnetic fields, see Ref. [22, 32].

Despite the apparent simplicity of the massive Dirac model, all observed transitions can be well-reproduced in the chosen range of low magnetic fields and also for all explored values of T (see Figs. 2f-j). Certain deviations appear in the region when transitions approach phonon lines (horizontal dotted lines in Figs. 2f-j) which are excluded from the fitting procedure. This allows us to extract the temperature dependence of v and Δ which are the only adjustable parameters of the used model (see Figs. 2k and l). The extracted values evolve smoothly and monotonously with temperature. The velocity parameter decreases slightly, which likely reflects only the unit cell increasing in size. This in turn implies a decrease in the overlap of atomic functions, and consequently, overall flattening of the band structure. The band gap gradually grows from the low-temperature value, $2\Delta = (5 \pm 1)$ meV, which is consistent with the preceding magneto-optical studies [19, 22, 32].

Interestingly, having established that the massive Dirac model is valid, one may infer the width of the band gap 2Δ, as well as its increase with T, directly from the

data in Figs. 2a-e without any fitting procedure. It simply corresponds to the separation between the lowest interband line ($0^- \to 1^+$ and $1^- \to 0^+$) and the fundamental CR mode ($0^+ \to 1^+$ and $1^- \to 0^-$). Other methods, presumably with a smaller resolution in energy, such as the ARPES or STM/STS techniques, provide us with the band gap larger by a factor of 3 or more [27–29, 35].

With increasing T, and above $T = 100$ K in particular, the observed interband inter-LL transitions visibly weaken, see Figs. 2a-e. This is partly due to thermally induced broadening of LLs, partly, when k_BT exceeds Δ, due to charge carriers excited thermally to LLs with higher indices. The latter reduces the transition strengths via the corresponding occupation factor. At low energies, the optical response becomes also modified by thermally excited carriers. With increasing T, the plasma edge forms gradually [19] and the simple one-electron picture is then no longer applicable. Instead, the observed CR mode starts to resemble, see Fig. 2e, the upper CR branch in the classical magneto-plasma response [36]: $\hbar(\omega_c^2 + \omega_p^2)^{1/2}$, where ω_p and ω_c are the screened plasma frequency and bare single-electron cyclotron frequency, respectively.

Let us now discuss implications of our experimental findings. Theoretical studies [11, 20, 37] suggest that bulk $ZrTe_5$ is a system close to a topological phase transition, which may, in fact, be the reason why no consensus about the topological nature of $ZrTe_5$ has so far been achieved. Theoretically, only a relatively small increase in the unit-cell volume is sufficient to bring $ZrTe_5$ from the STI to WTI regime, *i.e.*, from the inverted to the normal ordering of bands at the center of the Brillouin zone. Importantly, the band gap always closes and re-opens during such a topological phase transition.

Experimentally, it was shown that the unit-cell volume in $ZrTe_5$ increases monotonously with temperature [2]. Thanks to this, the temperature dependence of the band gap was proposed [20, 37] to be an unambiguous signature of the topological phase in $ZrTe_5$. In the STI regime, the band gap is first supposed to shrink with increasing T, then close completely, and finally, re-open in the WTI regime. In contrast, a monotonous increase of the band gap with temperature is expected in the WTI regime. Only the latter scenario is consistent with our data (Fig. 2g), thus implying the WTI phase in $ZrTe_5$. Let us note that the volume of the unit cell changes considerably in the explored range of temperatures, approximately by 0.5% [2].

Additional magneto-transport measurements, performed along with the magneto-reflectivity experiments, allowed us to correlate the evolution of the band gap width with the well-known resistivity anomaly in $ZrTe_5$. This effect refers to a characteristic peak in resistivity appearing when the temperature increases, see, *e.g.*, Refs. [5–10]. The temperature dependence of resistance of the explored sample measured during the first cool-down of the sample, $R_S(T)$, is plotted in Fig. 2m along with R_S values measured prior to the sweeps of our magneto-reflectivity measurements at a given fixed T. We speculate that the small discrepancies between the resistance values in the subsequent experiments, particularly visible at the peak value, could be due to a thermal-cycle-induced change in the contact resistance. This would modify the sourcing current, assumed to be constant while extracting resistance value. The observed profile, reaching maximum around $T_p \approx 75$ K is perfectly in-line with preceding experiments on samples with similar doping. In literature [24, 38], the appearance of resistivity anomaly in $ZrTe_5$ was sometimes associated with the temperature-driven closure of the band gap around T_p. Our data do not support such a conclusion.

In summary, we have extracted the temperature dependence of the band gap in $ZrTe_5$ using Landau level spectroscopy. We have found that the band gap increases monotonously, from the low-temperature value of $E_g = (5 \pm 1)$ meV to nearly 20 meV at $T = 140$ K. The observed behaviour is consistent with $ZrTe_5$ being a weak topological insulator.

ACKNOWLEDGMENTS

The work has been supported by the ANR projects DIRAC3D (ANR-17-CE30-0023) and COLECTOR (ANR-19-CE30-0032). A.A. acknowledges funding from the Swiss National Science Foundation through project PP00P2_202661. The authors also acknowledge the support of the LNCMI-CNRS in Grenoble, a member of the European Magnetic Field Laboratory (EMFL). The work at BNL was supported by the US Department of Energy, office of Basic Energy Sciences, contract no. DOE-sc0012704. This research was supported by the NCCR MARVEL, a National Centre of Competence in Research, funded by the Swiss National Science Foundation (grant number 205602).

Note added. During the review process, we learned about another magneto-optical study of $ZrTe_5$ study [39] presenting similar experimental results but suggesting a different interpretation.

[1] S. Furuseth, L. Brattas, and A. Kjekshus, Crystal structure of $HfTe_5$, Acta Chem. Scand. **27**, 2367 (1973).
[2] H. Fjellvag and A. Kjekshus, Structural properties of $ZrTe_5$ and $HfTe_5$ as seen by powder diffraction, Solid State Commun. **60**, 91 (1986).
[3] A. Smontara, K. Biljakovic, M. Miljak, and T. Sambongi, Thermal and magnetic measurements on $ZrTe_5$, Physica B+C **143**, 267 (1986).
[4] M. Izumi, T. Nakayama, K. Uchinokura, S. Harada, R. Yoshizaki, and E. Matsuura, Shubnikov-de Haas oscil-

lations and Fermi surfaces in transition-metal pentatellurides $ZrTe_5$ and $HfTe_5$, J. Phys. C: Solid State Phys. **20**, 3691 (1987).
[5] S. Okada, T. Sambongi, and M. Ido, Giant resistivity anomaly in $ZrTe_5$, Journal of the Physical Society of Japan **49**, 839 (1980).
[6] F. J. DiSalvo, R. M. Fleming, and J. V. Waszczak, Possible phase transition in the quasi-one-dimensional materials $ZrTe_5$ or $HfTe_5$, Phys. Rev. B **24**, 2935 (1981).
[7] E. Skelton, T. Wieting, S. Wolf, W. Fuller, D. Gubser, T. Francavilla, and F. Levy, Giant resistivity and X-ray diffraction anomalies in low-dimensional $ZrTe_5$ and $HfTe_5$, Solid State Commun. **42**, 1 (1982).
[8] T. M. Tritt, N. D. Lowhorn, R. T. Littleton, A. Pope, C. R. Feger, and J. W. Kolis, Large enhancement of the resistive anomaly in the pentatelluride materials $HfTe_5$ and $ZrTe_5$ with applied magnetic field, Phys. Rev. B **60**, 7816 (1999).
[9] C. Wang, Thermodynamically induced transport anomaly in dilute metals $ZrTe_5$ and $HfTe_5$, Phys. Rev. Lett. **126**, 126601 (2021).
[10] A. Gourgout, M. Leroux, J.-L. Smirr, M. Massoudzadegan, R. P. S. M. Lobo, D. Vignolles, C. Proust, H. Berger, Q. Li, G. Gu, C. C. Homes, A. Akrap, and B. Fauqué, Magnetic freeze-out and anomalous Hall effect in $ZrTe_5$, npj Quantum Mater. **7**, 71 (2022).
[11] H. Weng, X. Dai, and Z. Fang, Transition-metal pentatelluride $ZrTe_5$ and $HfTe_5$: A paradigm for large-gap quantum spin Hall insulators, Phys. Rev. X **4**, 011002 (2014).
[12] Q. Li, D. E. Kharzeev, C. Zhang, Y. Huang, I. Pletikosić, A. V. Fedorov, R. D. Zhong, J. A. Schneeloch, G. D. Gu, and T. Valla, Chiral magnetic effect in $ZrTe_5$, Nature Phys. **12**, 550 (2016).
[13] Y. Wang, H. F. Legg, T. Bömerich, J. Park, S. Biesenkamp, A. A. Taskin, M. Braden, A. Rosch, and Y. Ando, Gigantic magnetochiral anisotropy in the topological semimetal $ZrTe_5$, Phys. Rev. Lett. **128**, 176602 (2022).
[14] P. Li, C. H. Zhang, J. W. Zhang, Y. Wen, and X. X. Zhang, Giant planar Hall effect in the Dirac semimetal $ZrTe_5$, Phys. Rev. B **98**, 121108 (2018).
[15] F. Tang, Y. Ren, P. Wang, R. Zhong, J. Schneeloch, S. A. Yang, K. Yang, P. A. Lee, G. Gu, Z. Qiao, and L. Zhang, Three-dimensional quantum Hall effect and metal–insulator transition in $ZrTe_5$, Nature **569**, 537 (2019).
[16] S. Galeski, T. Ehmcke, R. Wawrzyńczak, P. M. Lozano, K. Cho, A. Sharma, S. Das, F. Küster, P. Sessi, M. Brando, R. Küchler, A. Markou, M. König, P. Swekis, C. Felser, Y. Sassa, Q. Li, G. Gu, M. V. Zimmermann, O. Ivashko, D. I. Gorbunov, S. Zherlitsyn, T. Förster, S. S. P. Parkin, J. Wosnitza, T. Meng, and J. Gooth, Origin of the quasi-quantized Hall effect in $ZrTe_5$, Nature Commun. **12**, 3197 (2021).
[17] Y. Zhou, J. Wu, W. Ning, N. Li, Y. Du, X. Chen, R. Zhang, Z. Chi, X. Wang, X. Zhu, P. Lu, C. Ji, X. Wan, Z. Yang, J. Sun, W. Yang, M. Tian, Y. Zhang, and H. kwang Mao, Pressure-induced superconductivity in a three-dimensional topological material $ZrTe_5$, PNAS **113**, 2904 (2016).
[18] R. Y. Chen, S. J. Zhang, J. A. Schneeloch, C. Zhang, Q. Li, G. D. Gu, and N. L. Wang, Optical spectroscopy study of the three-dimensional Dirac semimetal $ZrTe_5$, Phys. Rev. B **92**, 075107 (2015).
[19] E. Martino, I. Crassee, G. Eguchi, D. Santos-Cottin, R. D. Zhong, G. D. Gu, H. Berger, Z. Rukelj, M. Orlita, C. C. Homes, and A. Akrap, Two-dimensional conical dispersion in $ZrTe_5$ evidenced by optical spectroscopy, Phys. Rev. Lett. **122**, 217402 (2019).
[20] Z. Fan, Q.-F. Liang, Y. B. Chen, S.-H. Yao, and J. Zhou, Transition between strong and weak topological insulator in $ZrTe_5$ and $HfTe_5$, Sci. Rep. **7**, 45667 (2017).
[21] G. Manzoni, L. Gragnaniello, G. Autès, T. Kuhn, A. Sterzi, F. Cilento, M. Zacchigna, V. Enenkel, I. Vobornik, L. Barba, F. Bisti, P. Bugnon, A. Magrez, V. N. Strocov, H. Berger, O. V. Yazyev, M. Fonin, F. Parmigiani, and A. Crepaldi, Evidence for a strong topological insulator phase in $ZrTe_5$, Phys. Rev. Lett. **117**, 237601 (2016).
[22] Z.-G. Chen, R. Y. Chen, R. D. Zhong, J. Schneeloch, C. Zhang, Y. Huang, F. Qu, R. Yu, Q. Li, G. D. Gu, and N. L. Wang, Spectroscopic evidence for bulk-band inversion and three-dimensional massive Dirac fermions in $ZrTe_5$, PNAS **114**, 816 (2017).
[23] J. Mutch, W.-C. Chen, P. Went, T. Qian, I. Z. Wilson, A. Andreev, C.-C. Chen, and J.-H. Chu, Evidence for a strain-tuned topological phase transition in $ZrTe_5$, Science Advances **5**, eaav9771 (2019).
[24] B. Xu, L. X. Zhao, P. Marsik, E. Sheveleva, F. Lyzwa, Y. M. Dai, G. F. Chen, X. G. Qiu, and C. Bernhard, Temperature-driven topological phase transition and intermediate Dirac semimetal phase in $ZrTe_5$, Phys. Rev. Lett. **121**, 187401 (2018).
[25] J. Wang, Y. Jiang, T. Zhao, Z. Dun, A. L. Miettinen, X. Wu, M. Mourigal, H. Zhou, W. Pan, D. Smirnov, and Z. Jiang, Magneto-transport evidence for strong topological insulator phase in $ZrTe_5$, Nature Comm. **12**, 6758 (2021).
[26] L. Moreschini, J. C. Johannsen, H. Berger, J. Denlinger, C. Jozwiak, E. Rotenberg, K. S. Kim, A. Bostwick, and M. Grioni, Nature and topology of the low-energy states in $ZrTe_5$, Phys. Rev. B **94**, 081101 (2016).
[27] R. Wu, J.-Z. Ma, S.-M. Nie, L.-X. Zhao, X. Huang, J.-X. Yin, B.-B. Fu, P. Richard, G.-F. Chen, Z. Fang, X. Dai, H.-M. Weng, T. Qian, H. Ding, and S. H. Pan, Evidence for topological edge states in a large energy gap near the step edges on the surface of $ZrTe_5$, Phys. Rev. X **6**, 021017 (2016).
[28] X.-B. Li, W.-K. Huang, Y.-Y. Lv, K.-W. Zhang, C.-L. Yang, B.-B. Zhang, Y. B. Chen, S.-H. Yao, J. Zhou, M.-H. Lu, L. Sheng, S.-C. Li, J.-F. Jia, Q.-K. Xue, Y.-F. Chen, and D.-Y. Xing, Experimental observation of topological edge states at the surface step edge of the topological insulator $ZrTe_5$, Phys. Rev. Lett. **116**, 176803 (2016).
[29] H. Xiong, J. A. Sobota, S.-L. Yang, H. Soifer, A. Gauthier, M.-H. Lu, Y.-Y. Lv, S.-H. Yao, D. Lu, M. Hashimoto, P. S. Kirchmann, Y.-F. Chen, and Z.-X. Shen, Three-dimensional nature of the band structure of $ZrTe_5$ measured by high-momentum-resolution photoemission spectroscopy, Phys. Rev. B **95**, 195119 (2017).
[30] Y. Zhang, C. Wang, L. Yu, G. Liu, A. Liang, J. Huang, S. Nie, X. Sun, Y. Zhang, B. Shen, J. Liu, H. Weng, L. Zhao, G. Chen, X. Jia, C. Hu, Y. Ding, W. Zhao, Q. Gao, C. Li, S. He, L. Zhao, F. Zhang, S. Zhang, F. Yang, Z. Wang, Q. Peng, X. Dai, Z. Fang, Z. Xu, C. Chen, and X. J. Zhou, Electronic evidence of temperature-induced Lifshitz transition and topological

nature in $ZrTe_5$, Nature Comm. **8**, 15512 (2017).
[31] R. Y. Chen, Z. G. Chen, X.-Y. Song, J. A. Schneeloch, G. D. Gu, F. Wang, and N. L. Wang, Magnetoinfrared spectroscopy of Landau levels and Zeeman splitting of three-dimensional massless Dirac fermions in $ZrTe_5$, Phys. Rev. Lett. **115**, 176404 (2015).
[32] Y. Jiang, Z. L. Dun, H. D. Zhou, Z. Lu, K.-W. Chen, S. Moon, T. Besara, T. M. Siegrist, R. E. Baumbach, D. Smirnov, and Z. Jiang, Landau-level spectroscopy of massive Dirac fermions in single-crystalline $ZrTe_5$ thin flakes, Phys. Rev. B **96**, 041101 (2017).
[33] M. Orlita and M. Potemski, Dirac electronic states in graphene systems: optical spectroscopy studies, Semicond. Sci. and Technol. **25**, 063001 (2010).
[34] Y. Jiang, J. Wang, T. Zhao, Z. L. Dun, Q. Huang, X. S. Wu, M. Mourigal, H. D. Zhou, W. Pan, M. Ozerov, D. Smirnov, and Z. Jiang, Unraveling the topological phase of $ZrTe_5$ via magnetoinfrared spectroscopy, Phys. Rev. Lett. **125**, 046403 (2020).
[35] P. Zhang, R. Noguchi, K. Kuroda, C. Lin, K. Kawaguchi, K. Yaji, A. Harasawa, M. Lippmaa, S. Nie, H. Weng, V. Kandyba, A. Giampietri, A. Barinov, Q. Li, G. D. Gu, S. Shin, and T. Kondo, Observation and control of the weak topological insulator state in $ZrTe_5$, Nature Comm. **12**, 406 (2021).
[36] E. D. Palik and J. K. Furdyna, Infrared and microwave magnetoplasma effects in semiconductors, Rep. Prog. Phys. **33**, 1193 (1970).
[37] B. Monserrat and A. Narayan, Unraveling the topology of $ZrTe_5$ by changing temperature, Phys. Rev. Research **1**, 033181 (2019).
[38] Y. Tian, N. Ghassemi, and J. H. Ross, Dirac electron behavior and NMR evidence for topological band inversion in $ZrTe_5$, Phys. Rev. B **100**, 165149 (2019).
[39] Y. Jiang, T. Zhao, L. Zhang, Q. Chen, H. Zhou, M. Ozerov, D. Smirnov, and Z. Jiang, Canomalous temperature evolution of the Dirac band in $ZrTe_5$ across topological phase transition, preprint arXiv:2211.16711 (2022).

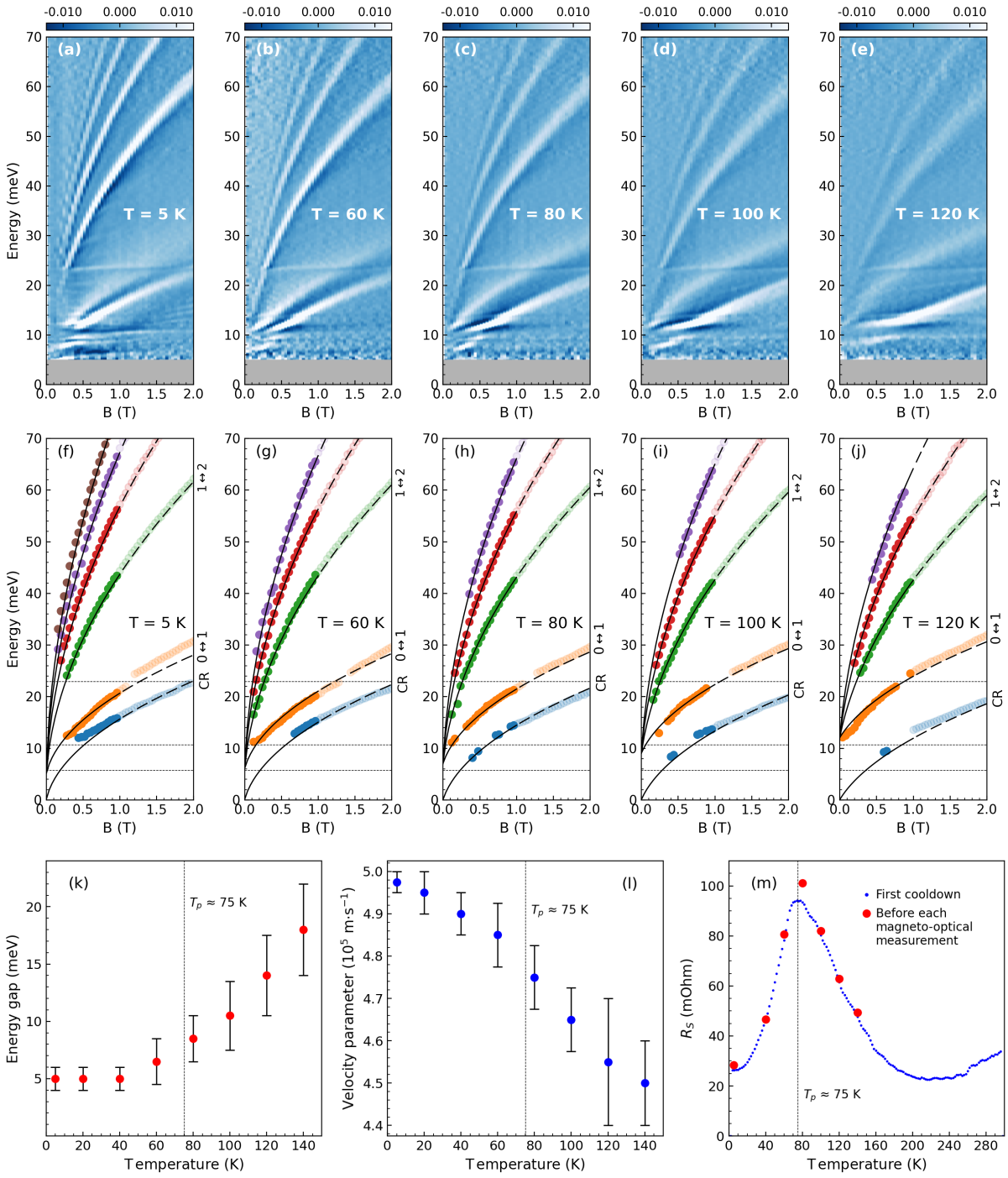


FIG. 2. (a-e) False-color plots of the first field-derivative of relative magneto-reflectivity, $d/dB[R_B/R_0]$, measured at the temperature of $T = 5, 60, 80, 100$ and 120 K. (f-j) The extracted positions of resonances at a given magnetic field and temperature. The solid lines represent the fits of interband inter-LL transitions for the data collected below 1 T. The dashed lines represent extrapolations of these fits to higher magnetic fields and energies. Dotted horizontal lines show energies of three most pronounced phonon modes (at 6, 11 and 23 meV) observed in Refs. [18, 19]. (k) The extracted energy band gap of $ZrTe_5$ as a function of temperature. (l) The experimentally determined temperature dependence of the effective velocity parameter. (m) The resistance anomaly in the explored $ZrTe_5$ sample, with the maximum of $R_S(T)$ around $T_p \approx 75$ K. The blue dots show the sample resistance during the first cool-down, the red circles before each run of the magneto-optical measurements at a given T. The temperature corresponding to the maximum in resistivity is marked by the vertical dashed lines in (k-m).